Monthly Notices
of the
ROYAL ASTRONOMICAL SOCIETY

Mon. Not. R. Astron. Soc. **413,** 908–920 (2011) doi:10.1111/j.1365-2966.2010.18185.x

Variability in quasar broad absorption line outflows – I. Trends in the short-term versus long-term data

D. M. Capellupo,[1⋆] F. Hamann,[1] J. C. Shields,[2] P. Rodríguez Hidalgo[3] and T. A. Barlow[4]

[1]*Department of Astronomy, University of Florida, Gainesville, FL 32611-2055, USA*
[2]*Department of Physics & Astronomy, Ohio University, Athens, OH 45701, USA*
[3]*Department of Astronomy and Astrophysics, Pennsylvania State University, University Park, PA 16802, USA*
[4]*Infrared Processing and Analysis Center, California Institute of Technology, Pasadena, CA 91125, USA*

Accepted 2010 December 9. Received 2010 December 9; in original form 2010 January 29

ABSTRACT

Broad absorption lines (BALs) in quasar spectra identify high-velocity outflows that likely exist in all quasars and could play a major role in feedback to galaxy evolution. The variability of BALs can help us understand the structure, evolution and basic physical properties of the outflows. Here we report on our first results from an ongoing BAL monitoring campaign of a sample of 24 luminous quasars at redshifts $1.2 < z < 2.9$, focusing on C IV λ1549 BAL variability in two different time intervals: 4–9 months (short term) and 3.8–7.7 yr (long term) in the quasar rest frame. We find that 39 per cent (7/18) of the quasars varied in the short-term data, whereas 65 per cent (15/23) varied in the long-term data, with a larger typical change in strength in the long-term data. The variability occurs typically in only portions of the BAL troughs. The components at higher outflow velocities are more likely to vary than those at lower velocities, and weaker BALs are more likely to vary than stronger BALs. The fractional change in BAL strength correlates inversely with the strength of the BAL feature, but does not correlate with the outflow velocity. Both the short-term and long-term data indicate the same trends. The observed behaviour is most readily understood as a result of the movement of clouds across the continuum source. If the crossing speeds do not exceed the local Keplerian velocity, then the observed short-term variations imply that the absorbers are <6 pc from the central quasar.

Key words: galaxies: active – quasars: absorption lines – quasars: general.

1 INTRODUCTION

Accretion disc outflows play a key role in the physics of quasars and their environs. Quasar outflows may be an integral part of the accretion process and the growth of supermassive black holes (SMBHs), by allowing the accreting material to release angular momentum. These outflows may also provide enough kinetic energy feedback to have an effect on star formation in the quasar host galaxies, to aid in 'unveiling' dust-enshrouded quasars and to help distribute metal-rich gas to the intergalactic medium (e.g. Di Matteo et al. 2005; Moll et al. 2007).

The location and three-dimensional structure of quasar outflows are poorly understood. Sophisticated models have been developed that envision these outflows as arising from a rotating accretion disc, with acceleration to high speeds by radiative and/or magnetocentrifugal forces (Murray et al. 1995; Proga & Kallman 2004; Everett 2005; Proga 2007). Improved observational constraints are needed to test these models and allow estimation of mass-loss rates, kinetic energy yields and the role of quasar outflows in feedback to the surrounding environment. In this paper, we focus on the most prominent signatures of accretion disc outflows that appear in quasar spectra, the broad absorption lines (BALs). BALs are defined to have velocity widths $>2000\,\mathrm{km\,s^{-1}}$ at absorption depths >10 per cent below the continuum (Weymann et al. 1991), and they appear in the spectra of ∼10–15 per cent of quasars (Reichard et al. 2003a; Trump et al. 2006). Since only a fraction of quasar spectra display these features, the presence of BALs could represent a phase in the evolution of a quasar and/or particular orientations where the outflow lies between us and the quasar emission sources. Other studies have found support for the latter scenario, given the similarity of various properties between BAL quasi-stellar objects (BAL QSOs) and non-BALQSOs (e.g. Weymann et al. 1991; Shen et al. 2008).

⋆E-mail: dancaps@astro.ufl.edu

Studying the variability in these absorption features can provide important insight into the structure and dynamics of the outflows. For example, we can use information about short-term variability to place constraints on the distance of the absorbing material from the central SMBH. The more quickly the absorption is varying, the closer the absorber is to the central source, based on nominally shorter crossing times for moving clouds (Hamann et al. 2008 and Section 5 below) or the higher densities required for shorter recombination times (Hamann et al. 1997). Long-term variability measurements provide information on the homogeneity and stability of the outflow. A lack of variability on long time-scales implies a smooth flow with a persistent structure. General variability results provide details on the size, kinematics and internal makeup of substructures within the flows. Variability studies can also address the evolution of these outflows as the absorption lines are seen to come and go, or one type of outflow feature evolves into another (e.g. Hamann et al. 2008).

A small number of previous studies have investigated variability in BALs, emphasizing C IV λ1549 because of its prominence and ease of measurement. Barlow (1993) carried out a study of 23 BALQSOs, covering time-scales of $\Delta t \lesssim 1$ yr.[1] Lundgren et al. (2007) used Sloan Digital Sky Survey (SDSS) spectra of 29 quasars to study C IV BAL variability on similar time-scales. Gibson et al. (2008) studied variability on longer time-scales (3–6 yr) by combining data for 13 BALQSOs from the Large Bright Quasar Survey (LBQS) and SDSS. Gibson et al. (2010) reports on variability on multimonth to multiyear time-scales, using 3–4 epochs of data for nine BALQSOs. They also compare variability in Si IV absorption to variability in C IV absorption in their sample.

In the present study, we go beyond existing work by carrying out a monitoring programme of BALQSOs from the sample of Barlow (1993). This strategy provides BAL variability data covering longer time-scales as well as a wider range in time-scales within individual sources. We include archival spectra from the SDSS, when available, to augment the temporal sampling. This paper reports our results for C IV λ1549 variability with measurements selected to enable comparison between short-term (0.35–0.75 yr) behaviour and long-term (3.8–7.7 yr) behaviour. We identify trends in the data with velocity and the depth of the absorption. We avoid using equivalent width (EW) measurements, which can minimize a change that occurs in a portion of a much wider trough. In subsequent papers, we will discuss variability properties in the entire data set, including more epochs on individual quasars, sampling in a much shorter time domain and comparisons between the C IV and Si IV λ1400 variabilities to place constraints on the outflow ionizations and column densities. Section 2 below discusses the observations and the quasar sample. Section 3 describes the steps we followed to identify the C IV BALs and where they varied. Section 4 describes our results, and Section 5 discusses the implications of these results with comparisons to previous work.

2 DATA AND QUASAR SAMPLE

Between 1988 and 1992, Barlow (1993) and his collaborators (e.g. Barlow et al. 1992) obtained spectra for 28 BALQSOs with the Lick Observatory 3-m Shane Telescope. They obtained multiepoch spectra for 23 of these quasars for a study of short-term BAL variability. They selected these objects from already known BALQSOs, with redshifts of 1.2–2.9. When selecting objects for their monitoring programme, they gave preference to quasars known to have either absorption line or photometric variability. However, in most cases, this information was not available, and they selected more quasars at higher redshifts due to higher detector sensitivity at longer wavelengths. While this sample of BALQSOs is not randomly selected, it does cover a wide range of BAL strengths (see Table 1 and Fig. 1).

Barlow (1993) used the Lick Observatory Kast spectrograph to obtain spectra with settings for high resolution, $R \equiv \lambda/\Delta\lambda \approx 1300$ (230 km s^{-1}), and moderate resolution, $R \approx 600$ (530 km s^{-1}). Most of the objects were observed at both settings. For our analysis of these data discussed below, we used the high-resolution observations for most sources. In some cases, only a moderate-resolution observation is available or choosing the high-resolution observation would compromise wavelength coverage. Since BALs have a width of at least 2000 km s^{-1}, a resolution of 530 km s^{-1} is sufficient to detect changes in their profiles.

Starting in 2007 January, we have been using the MDM Observatory 2.4-m Hiltner Telescope to re-observe the BALQSOs in the sample of Barlow (1993), with the goal of monitoring BAL variability over a wide range of time-scales, from <1 month to nearly 8 yr. We also supplemented our data set with spectra from the SDSS. So far, we have over 120 spectra for 24 BALQSOs, and we continue to collect more data. We note that two of these objects are not strictly BALQSOs because they have a balnicity index of zero (see Section 3.2 below). None the less, we include them in our sample because they do have broad absorption features at velocities that we include in our variability analysis (Section 3.3).

We used the MDM CCDS spectrograph with a 350 groove per millimetre grating in first order and a 1 arcsec slit to yield a spectral resolution of $R \approx 1200$ (250 km s^{-1}), with wavelength coverage of ∼1600 Å. The spectrograph was rotated between exposures to maintain approximate alignment of the slit with the parallactic angle, to minimize wavelength-dependent slit losses. The wavelength range for each observation was determined based on the redshift of the target quasar such that the coverage was blue enough to include the Lyα emission and red enough to include the C IV emission feature. The co-added exposure times were typically 1–2 h per source.

We reduced the data using standard reduction techniques with the IRAF[2] software. The data are flux calibrated on a relative scale to provide accurate spectral shapes. Absolute flux calibrations were generally not obtained due to weather or time constraints.

The SDSS is an imaging and spectroscopic survey of the sky at optical wavelengths. The data were acquired by a dedicated 2.5-m telescope at Apache Point Observatory in New Mexico. The spectra cover the observer-frame optical and near-infrared, from 3800 to 9200 Å, and the resolution is $R \approx 2000$ (150 km s^{-1}). For spectra, typically three exposures were taken for 15 min each, and more exposures were taken in poor conditions to achieve a target signal-to-noise ratio. The multiple observations were then co-added (Adelman-McCarthy et al. 2008). The SDSS includes observations of 11 of the quasars in the Lick sample. However, three of the SDSS observations are unusable because the redshifts of those quasars are too low for the C IV BALs to appear in the SDSS spectra. Therefore,

[1] Throughout this paper, all time intervals are measured in years in the rest frame of the quasar.

[2] The Image Reduction and Analysis Facility (IRAF) is distributed by the National Optical Astronomy Observatories (NOAO), which is operated by the Association of Universities for Research in Astronomy (AURA), Inc., under cooperative agreement with the National Science Foundation.

Table 1. Quasar data and C IV variability results.

Coord. (1950.0)	Name	z_{em}	BI	Short term Obs. 1	Short term Obs. 2	Short term Δt	Short term Vary?	Long term Obs. 1	Long term Obs. 2	Long term Δt	Long term Vary?
0019+0107	UM 232	2.13	2290	1989.84	1991.86	0.65	N	1989.84	2007.04	5.50	N
0043+0048	UM 275	2.14	4330	2000.69	2001.79	0.35	N	1991.86	2008.03	5.15	Y
0119+0310	AD85 D08	2.09	5170	1989.85[a]	1991.86	0.65	Y	1989.85[a]	2007.07	5.57	Y
0146+0142	UM 141	2.91	5780	1988.93[a]	1991.86	0.75	Y	1988.93[a]	2007.05	4.64	Y
0226−1024	WFM91 0226−1024	2.25	7770					1991.87	2007.04	4.66	Y
0302+1705	HB89 0302+170	2.89	0					1989.84[a]	2007.05	4.42	N
0842+3431	CSO 203	2.15	4430	2007.04	2008.35	0.42	Y	1990.90	2008.35	5.54	N
0846+1540	H 0846+1540	2.93	0	1990.16	1992.19	0.52	Y	1992.19	2007.05	3.78	Y
0903+1734	HB89 0903+175	2.77	10 700	2006.31	2008.28	0.52	Y	1989.26[a]	2008.28	5.04	Y
0932+5006	SBS 0932+501	1.93	7920	1989.84	1991.10	0.43	N	1989.84	2008.28	6.30	Y
0946+3009	PG 0946+301	1.22	5550	1991.10	1992.23	0.51	Y	1991.10	2008.28	7.74	Y
0957−0535	HB89 0957−055	1.81	2670	1990.89	1992.32	0.51	N	1992.32	2008.35	5.70	N
1011+0906	HB89 1011+091	2.27	6100	2007.07	2008.35	0.39	N	1992.19	2008.35	4.94	Y
1232+1325	HB89 1232+134	2.36	11 000					1989.26[a]	2008.03	5.58	N
1246−0542	HB89 1246−057	2.24	4810	2007.04	2008.35	0.40	N	1992.19	2008.35	4.99	Y
1303+3048	HB89 1303+308	1.77	1390	2007.04	2008.28	0.45	N	1992.32	2008.28	5.76	Y
1309−0536	HB89 1309−056	2.22	4690					1992.19	2007.04	4.61	N
1331−0108	UM 587	1.88	10 400	2007.04	2008.28	0.43	N	1992.32	2008.28	5.55	Y
1336+1335	HB89 1336+135	2.45	7120					1989.26[a]	2008.28	5.52	N
1413+1143	HB89 1413+117	2.56	6810	2006.31	2008.28	0.55	Y	1989.26[a]	2008.28	5.35	Y
1423+5000	CSO 646	2.25	3060	2007.07	2008.35	0.39	N	1992.32	2008.35	4.93	N
1435+5005	CSO 673	1.59	11 500					1992.19	2008.35	6.25	Y
1524+5147	CSO 755	2.88	2490	1989.60	1991.52	0.49	N	1991.52	2008.28	4.32	Y
2225−0534	HB89 2225−055	1.98	7920	1988.46	1989.84	0.46	N				

[a]These Lick observations were taken at the lower resolution setting ($R \approx 600$; see Section 2).

we have usable SDSS spectra for eight of the objects in our sample, and they were taken between 2000 and 2006.

3 ANALYSIS

3.1 Short-term and long-term data sets

From the data in our BAL monitoring campaign, for each object, we select one pair of observations for the short-term analysis and one pair for the long-term analysis. For the long-term analysis, we want the longest time baseline possible. The first observation for each object is the earliest Lick observation with the highest available resolution as well as wavelength coverage that extends from the Lyα emission line through the C IV emission line. For the second observation for each object, we use the most recent MDM spectrum. We have long-term data for 23 objects, with resulting Δt of 3.8–7.7 yr. We note that for certain objects, the redshift is low enough that the Lyα emission line is not shifted into the wavelength coverage of our data and therefore is not present in some of the spectra (e.g. 0946+3009).

For the short-term analysis, the range in the values of Δt among the objects should be small while including as many objects as possible. The best compromise we found was a range for Δt of 0.35–0.75 yr, which allows us to include 18 objects in the short-term analysis. In order to include this many objects, we use data for some objects that only cover the region from the Si IV emission to the C IV emission, which is sufficient for the analysis in this paper. These observations were selected separately from the long-term epochs and were chosen to fit into this Δt interval. These observations were taken before or at any time in between the two long-term observations. There is one object for which we have short-term Lick data, but no long-term data (2225−0534), so we have in total 24 objects in our full sample.

3.2 Characterizing the quasar sample

Table 1 summarizes our full sample of long-term and short-term data, as described above. The first four columns provide information on all 24 quasars. z_{em} is the emission redshift[3] and BI is the 'balnicity index', as described below. The remaining columns are separated into the short-term analysis and long-term analysis. The columns with 'vary?' have either Yes or No values to indicate variability anywhere in the C IV troughs (refer to Section 4) and Δt is the time difference (in years) in the quasar frame between observations. The observations from 1988 to 1992 are from Lick, the observations from 2000 to 2006 are from SDSS and the observations from 2007 to 2008 are from MDM.

Fig. 1 contains spectra for all 24 objects, showing the long-term comparisons between a Lick spectrum and an MDM spectrum. The one exception is 2225−0534, for which we only have short-term Lick data. The velocity scale is based on the wavelength of C IV in the observed frame calculated from the redshifts given in Table 1. We use a weighted average of the C IV doublet wavelengths, i.e. 1549.05 Å.

The balnicity index (BI; Weymann et al. 1991) is designed to differentiate between BALQSOs and non-BALQSOs and provide a measure of the BAL strength, expressed as an EW in units of velocity. It quantifies absorption that is blueshifted between −3000 and −25 000 km s^{-1} from the C IV emission-line centre, is at least ∼10 per cent below the continuum and is wider than 2000 km s^{-1}. By this definition, if a quasar has a BI greater than zero, then it is classified as a BALQSO. The highest possible value of BI is 20 000.

[3] The values of z_{em} were obtained from the NASA/IPAC Extragalactic Data base (NED), which is operated by the Jet Propulsion Laboratory, California Institute of Technology, under contract with the National Aeronautics and Space Administration.

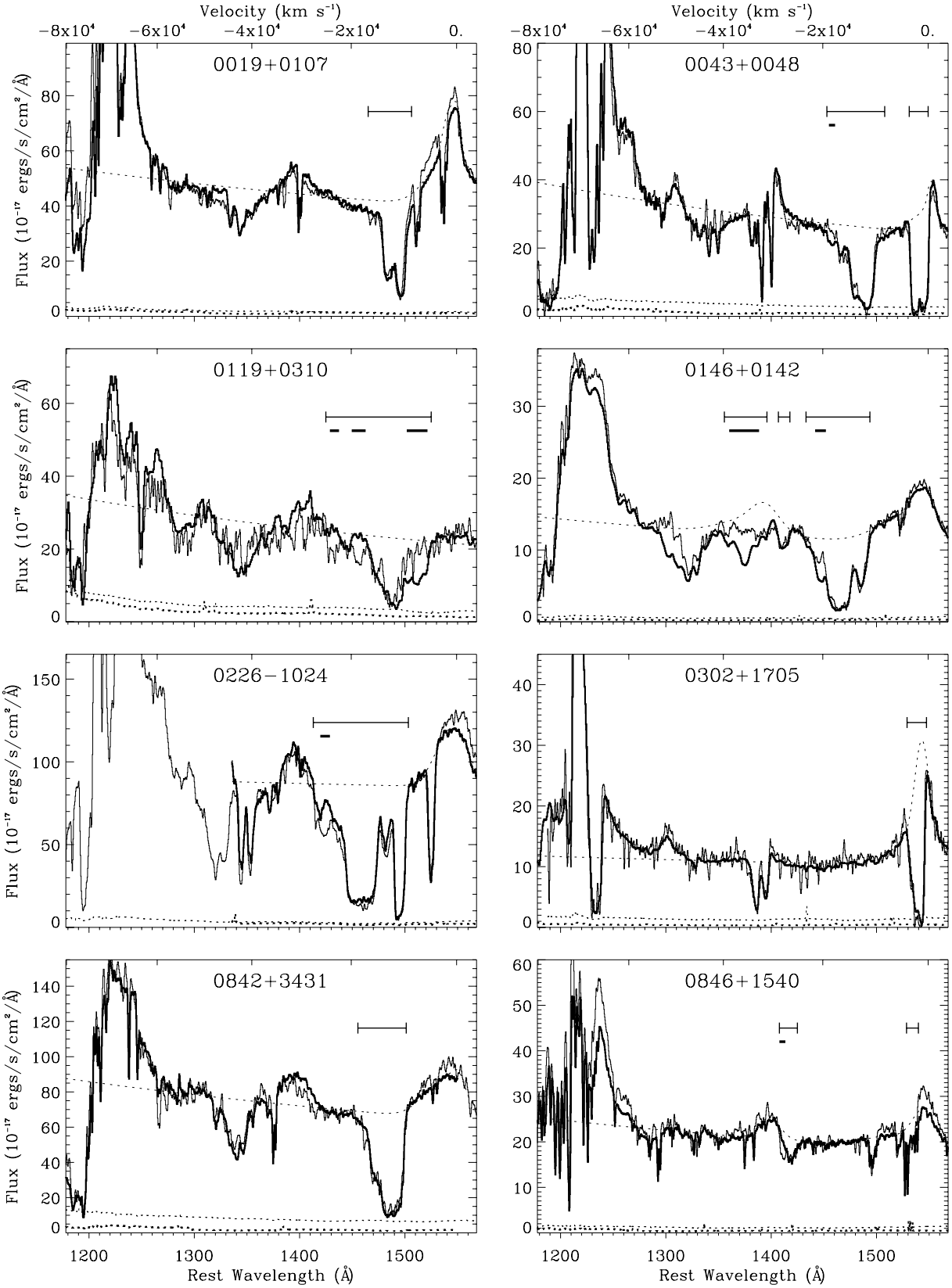

Figure 1. Smoothed spectra of all 24 quasars in our sample, showing the long-term comparisons between a Lick Observatory spectrum (bold curves) and the most recent MDM data (thin curves). The one exception is 2225−0534, for which we only have short-term data (see Table 1). The vertical flux scale applies to the Lick data, and the MDM spectrum has been scaled to match the Lick data in the continuum. The dashed curves show our pseudo-continuum fits. The thin horizontal bars indicate intervals of BAL absorption included in this study, and the thick horizontal bars indicate intervals of variation within the BALs. The formal 1σ errors are shown near the bottom of each panel.

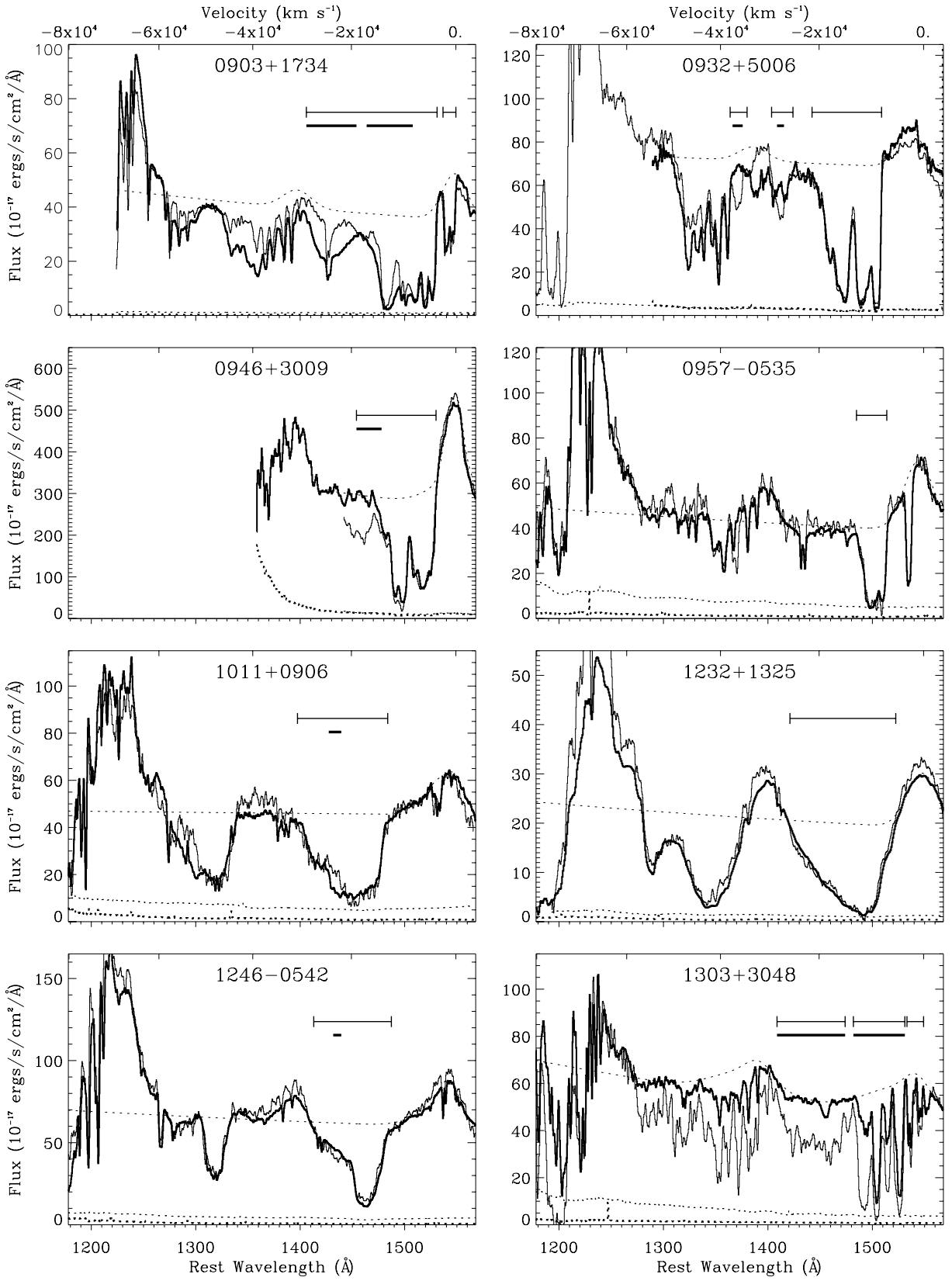

Figure 1 – *continued*

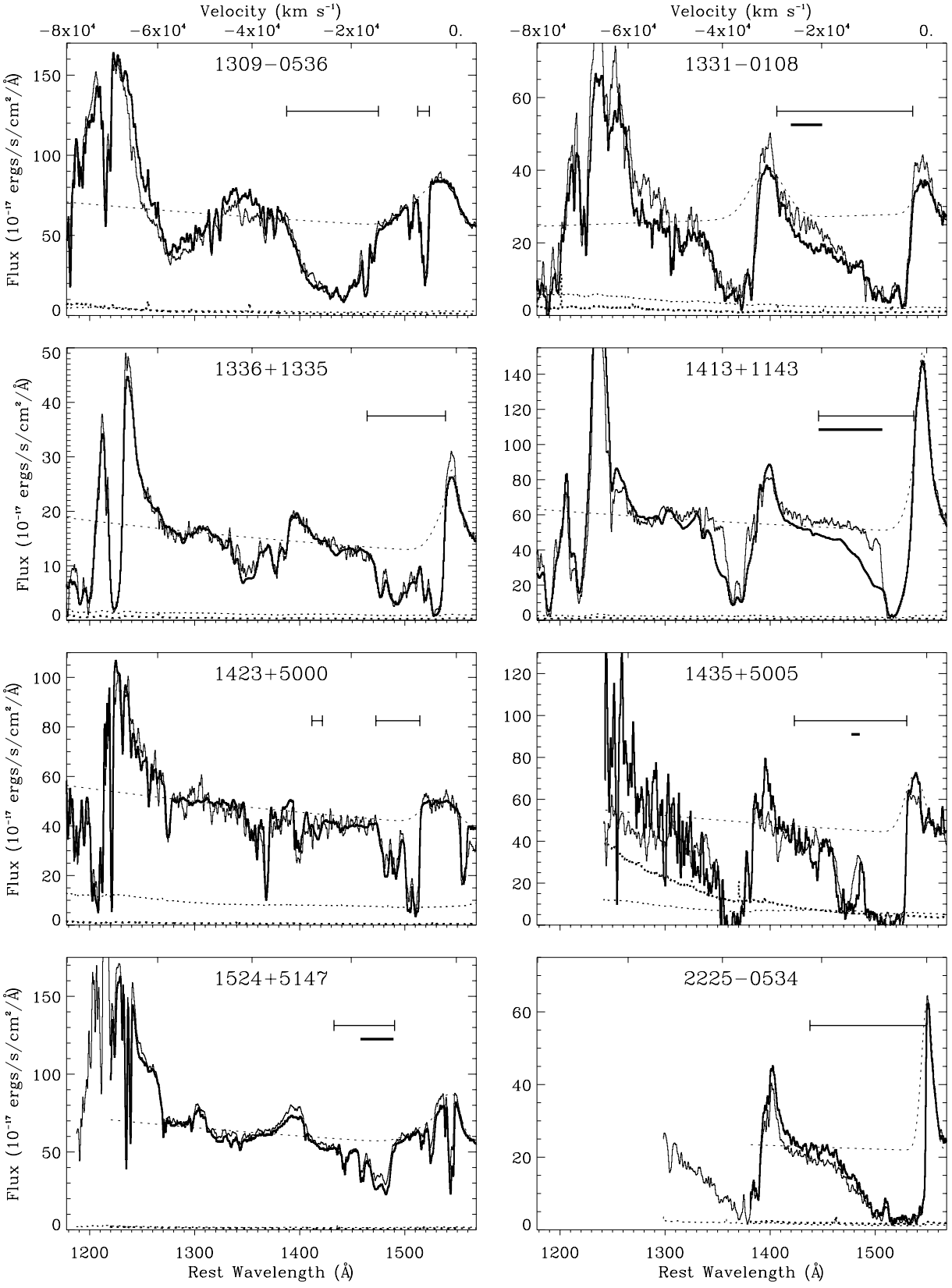

Figure 1 – *continued*

We measure BI in one observation per object to characterize the sample and allow for comparison with BALQSOs in other studies. We do not use BI in our variability analysis. In order to normalize the spectra and measure BI, and later absorption strength (see Section 3.3), we first had to fit a pseudo-continuum to one spectrum per quasar, which includes the quasar's continuum emission plus the broad emission lines (BELs). We adopt the Lick observations used in the long-term analysis as our fiducial epoch for which we fit the pseudo-continua and measure BI. We constructed this pseudo-continuum by fitting a power law to the continuum away from any emission or absorption lines, and then adding to that an estimate of the C IV and, if necessary, the Si IV BEL profiles.[4] To fit the continuum, we fit a power-law function to two regions on the spectrum that are free of strong emission lines. The preferred wavelength ranges for the fits were 1270–1350 Å and 1680–1800 Å. These ranges were adjusted to avoid emission and absorption features as much as possible or due to the limits of the wavelength coverage. Fitting the C IV emission is complicated by, for example, potential asymmetries in the emission profiles and absorption in the emission region (e.g. Reichard et al. 2003b). Therefore, we are flexible in our fitting routine, using between 1 and 3 Gaussians to define the line profile. The Gaussians have no physical meaning, and we simply use them for obtaining a reasonable fit to the profile. If there is any absorption on top of the emission, we ignore those wavelengths when defining the fit. In cases where the absorption is wide enough that it obscures up to half of the emission line (e.g. 1413+1143), we assume the emission line is symmetric. In cases where the Gaussian, or multiple-Gaussian, fit did not provide the right shape and we have enough information about the profile (e.g. 1423+5000), we manually adjusted the fit to better match the C IV emission line.

For quasars where the C IV absorption is at a velocity that overlaps the Si IV emission, we also fit the Si IV emission line. If most, or all, of the Si IV emission feature is absorbed, we synthesized a Si IV profile by taking the C IV fit, shifting its centre wavelength to the location of Si IV, adjusting the full width at half-maximum (given the wider separation between the Si IV doublet lines) and scaling the emission strength by a factor of 0.342. This scalefactor is based on composite quasar spectra from which Vanden Berk et al. (2001) found the typical strength of various emission lines. We relied on this scalefactor in cases such as 0146+0142, where we have little information about the Si IV emission line. Otherwise, in a case such as 0846+1540, we fit between 1 and 3 Gaussians to the Si IV line, as we did for the C IV emission, because we have more information about the profile of the Si IV emission line. The pseudo-continuum fits for each object are shown by the smooth dotted curves in Fig. 1.

3.3 Measuring the BAL variability

For each quasar, we compare the two spectra in our short-term and long-term intervals (see Table 1) to search for variability in the C IV BALs. First, we determined the velocity ranges over which BAL absorption occurs. These ranges might differ between the two observing epochs. We therefore set the range to the extremes observed in either epoch. Our definition of these ranges is guided by the definition of BI, i.e. they must present contiguous absorption reaching $\geq$10 per cent below the continuum across $\geq$2000 km s^{-1}. We do not follow the requirement that the absorption be blueshifted between -3000 and $-25\,000$ km s^{-1} because we want to include all C IV broad absorption in our analysis (as a result, our sample contains two objects, 0302+1705 and 0846+1540, with a BI of 0). In general, the C IV BALs occur between the Si IV and C IV emission lines, but some of the C IV absorption is blueshifted enough that it appears bluewards of the Si IV emission-line centre (e.g. 0146+0142). In these cases, we can confirm that the absorption bluewards of the Si IV emission line is due to C IV, and not Si IV, because any significant Si IV absorption should be accompanied by C IV absorption at the same velocity. This is evident from numerous observations of BALQSOs, where the Si IV and C IV absorptions are clearly identified (e.g. fig. 1, Korista et al. 1993), and from theoretical considerations of the relative strengths of these lines (Hamann et al. 2008). Our sample includes broad absorption troughs from 0 to $-40\,000$ km s^{-1}.

In order to compare any two spectra for variability in the defined absorption ranges, we scaled the spectra so that regions free of absorption and emission in each spectrum match. This is necessary because of uncertainties in the flux calibration and possible real changes in the quasar emissions. We applied a simple vertical scaling so that the spectra from each epoch match the fiducial Lick spectrum along the continuum redwards of the C IV emission feature (i.e. from 1560 Å to the limit of the wavelength coverage), between the Si IV and C IV emission ($\sim$1425–1515 Å) and between the Lyα and the Si IV emission ($\sim$1305–1315 Å). In nearly all cases, a simple scaling produced a good match between the spectra from different epochs. The results for the two long-term epochs are shown in Fig. 1. In some cases, however, there were disparities in the overall spectral shape of the two spectra. To remove these disparities, we fitted either a linear function (for 0903+1734, 1413+1143 and 1423+5000) or quadratic function (for 0019+0107 and 1309−0536) to the spectral regions that avoid the BALs in a ratio of the two spectra. We then multiplied this function by the comparison spectrum.

We identify BAL variability in velocity intervals that correspond to at least two resolution elements in the lower resolution Lick spectra, i.e. 1200 km s^{-1}. Our procedure to identify variability intervals relies mainly on visual inspection because photon statistics alone are not sufficient for defining real variability. Most of the occurrences of variability recorded for this study are obvious by simple inspection. However, we also examined all cases of weak or possible variability to ensure that no occurrences of significant real variability are missed. We determined the significance of variability based on two criteria. First, we calculate the average flux and associated error within each variability interval and use that to place an error on the flux differences between the two spectra. We include in this study only the intervals of variability where the flux differences are at least 4σ. We emphasize that all of the intervals which varied by 4σ or more are readily identified by our initial inspection technique. Therefore, there is no danger of variable intervals being missed. However, the 4σ threshold alone can include spurious or highly uncertain variability results because of uncertainties not captured by the photon statistics. These additional uncertainties can arise from the flux calibration, a poorly constrained continuum placement, underlying emission-line variability or our reconstruction of a severely absorbed emission-line profile. We therefore apply a second significance criterion based on our assessment of these additional uncertainties. We take a conservative approach by excluding variability intervals where the additional uncertainties might be large (even if the flux difference passes the formal 4σ threshold described above). This second criterion caused the exclusion of just a few intervals. See below for examples. The velocity intervals finally classified as

[4] Note that the feature we attribute to Si IV may also include O IV] λ1400 emission.

variable in the long-term data are indicated by bold horizontal lines in Fig. 1.

To help clarify our assessments of the additional uncertainties, we point out some specific velocity intervals that pass the 4σ threshold and appear variable by casual inspection, but are none the less excluded from our analysis because the additional uncertainties are significant. For example, in 1246−0542, we do not include the region around $-17\,000\,\mathrm{km\,s^{-1}}$ because the noise level in that portion of the trough makes it a very tenuous candidate for inclusion in the study. The region around $-21\,000\,\mathrm{km\,s^{-1}}$ in 1435+5005 is a similar case because here the increased noise level of the spectra towards greater outflow velocities makes a determination of variability more uncertain. We note that the increased scatter in the data for these two objects is less notable in the smoothed spectra plotted in Fig. 1. In a couple cases, a slight difference in the slope between two comparison spectra adds some uncertainty. In 1413+1143, the blue wing of the C IV trough in the MDM spectrum extends slightly above the defined continuum. This may be due to some anomaly in the flux calibration, so we define the blue end of the BAL (and the variability interval) as $-20\,600\,\mathrm{km\,s^{-1}}$. In 2225−0534, there is very little continuum available for matching the two comparison spectra, and this added uncertainty makes the small flux difference at the bluest portion of the BAL trough too tenuous to be included. A slight difference in slope between the two epochs could be responsible for any apparent changes in the wing of this BAL, and we do not have enough visible continuum to discount this possibility.

Identifying variability in the spectral regions which overlap the C IV and Si IV emission lines is further complicated by possible variability in the emission lines themselves (e.g. Wilhite et al. 2005). We record BAL variability in these spectral regions only if it is large compared to any reasonable change in the BELs and/or the absorption changes abruptly over just portions of a BEL profile. For example, in 0146+0142, the interval from $-38\,800$ to $-32\,700\,\mathrm{km\,s^{-1}}$ clearly shows BAL absorption weakening to approximately continuum level. In another case, 0932+5006, we include the intervals from $-37\,500$ to $-35\,400\,\mathrm{km\,s^{-1}}$ and $-28\,400$ to $-27\,000\,\mathrm{km\,s^{-1}}$ because there is clearly BAL absorption there in the MDM spectrum. We did not attribute the change in flux from approximately $-34\,000$ to $-30\,000\,\mathrm{km\,s^{-1}}$ to a BAL because it is unclear what is the primary cause of variability in this interval. While the identifications of BAL absorption and variability in the regions overlapping C IV and Si IV emission are secure, the measurements of absorption strength ($\langle A\rangle$; see below) in this region have added uncertainty since fitting the emission lines is more uncertain than fitting the continuum. When looking at correlations with velocity in this study, we identify trends using all the data, but also confirm the existence of these trends in the velocity range $-27\,000$ to $-8000\,\mathrm{km\,s^{-1}}$, which avoids the emission lines. For correlations with absorption strength (see below), since there are few cases of variability at the extremes of the examined velocity range, their inclusion does not significantly alter the plots or the final results.

In order to look for trends in the data, we calculated the absorption strength as a function of velocity in each spectrum. We first normalized each spectrum using the pseudo-continuum fit (see Section 3.2) for that quasar. We can apply the pseudo-continua derived in Section 3.2 to the other epochs for each quasar because those epochs have already been scaled to match the fiducial Lick spectrum. However, we adjust the emission-line fits in cases where the emission line varied. We define absorption strength, A, as the fraction of the normalized continuum flux removed by absorption ($0 \leq A \leq 1$) within a specified velocity interval. A single A value is adopted for each velocity interval based on the average flux within that interval. If there is variability, then the absorption strength changed, and we calculate the average absorption strength, $\langle A\rangle$, and the change in absorption strength, ΔA, between the two epochs being compared. The velocity intervals used to calculate $\langle A\rangle$ and ΔA are defined to (i) include only portions of the spectrum with BAL absorption and (ii) clearly separate the spectral regions within BAL troughs that did and did not vary. Specifically, the variable and non-variable absorption regions are each divided into equal-sized bins, with a bin width of 1000 to $2000\,\mathrm{km\,s^{-1}}$ depending on the velocity width of the region. This strategy makes the bin widths used to measure $\langle A\rangle$ and ΔA similar to the nominal width of $1200\,\mathrm{km\,s^{-1}}$ used above while providing the flexibility needed to begin and end at the boundaries defined above between absorbed/unabsorbed and variable/non-variable spectral regions. In each of these velocity bins, we also calculate the fractional change in the absorption strength, $|\Delta A|/\langle A\rangle$, which can have values from 0 to 2. Spectral regions that did not vary according to the criteria described above have ΔA set to zero automatically. Note that, with $\langle A\rangle$ and ΔA determined in this way, each quasar can contribute more than once to these quantities in our variability analysis, depending on the range of strengths and velocities covered by its BAL troughs, because each bin showing variability is treated as a separate occurrence. We plot the relationship between absorption strength, $\langle A\rangle$, and outflow velocity for all the quasars in our long-term subsample in Fig. 2. A correlation between these two quantities will have implications for our results when we compare variability measures to each of these quantities individually (see Sections 4 and 5). There is a trend for lower values of $\langle A\rangle$ at increasing outflow velocity, which is especially apparent from $-27\,000$ to $-8\,000\,\mathrm{km\,s^{-1}}$, away from the regions of Si IV and C IV emission. The errors in the individual points are much smaller ($\sigma_{\langle A\rangle} \leq 0.01$) than the dispersion of points in each bin. However, the bins at $< -30\,000\,\mathrm{km\,s^{-1}}$ only contain one or two quasars, so the average $\langle A\rangle$ in those bins can be uncertain by up to a factor of 2, given the additional uncertainty of fitting the Si IV emission line. The weaker absorption found at higher velocities in our sample is consistent with absorption in the mean BAL spectra constructed by Korista et al. (1993).

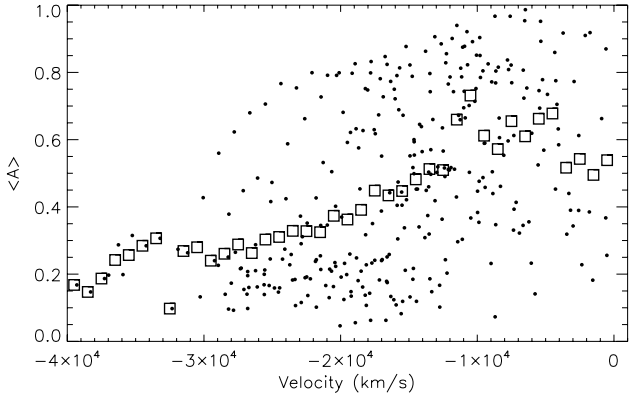

Figure 2. The average normalized absorption strength ($\langle A\rangle$), calculated throughout all of the BALs in the quasars in our long-term subsample, as a function of the outflow velocity of the absorbing material. The individual points in each bin (with width $1000\,\mathrm{km\,s^{-1}}$) represent the $\langle A\rangle$ for a single quasar, and the open squares represent the average of all points in that bin.

4 RESULTS

Table 1 indicates whether there was significant variability in the C IV BALs of each quasar in the short-term and long-term data. We

found that 39 per cent (7/18) of quasars with short-term data varied, whereas in the long term, 65 per cent (15/23) varied. One quasar varied only in the short-term data, so combining both short-term and long-term data, 67 per cent (16/24) of the quasars varied overall.

We investigated C IV BAL variability as a function of outflow velocity. Using the velocity ranges for each quasar where we have identified absorption and variability (Section 3.3), we count how many quasars have BAL absorption and variability in each velocity bin. In Fig. 3, the top two panels show the number of quasars with C IV BAL absorption and the number with C IV BAL variability at each velocity. The third panel is the second panel divided by the top one, which gives the fraction of C IV BALs that varied at each velocity. The dashed, dotted and solid curves indicate results for the long-term, short-term and combined data set comparisons, respectively. The plot implies that BALs at higher velocities are more likely to vary than those at lower velocities.

The bottom panel in Fig. 3 displays 1σ error bars based on Wilson (1927) and Agresti & Coull (1998). These errors are based on counting statistics for the number of quasars with absorption and variability at each velocity. We perform a least-squares fit to confirm that a correlation exists between incidence of variability and velocity. The slope of the combined data is $-1.51 \pm 0.25 \times 10^{-5}$, in the formal unit, fraction per km s^{-1}. The slope is non-zero at a 6σ significance. If we repeat the least-squares fit with only the bins with the most data (bins containing at least eight quasars with absorption), the slope is $-1.76 \pm 0.33 \times 10^{-5}$ fraction per km s^{-1}, which is non-zero at a 5σ significance. Using this restriction limits the fit to only the data from $-29\,000$ to -2000 km s^{-1}. We perform the least-squares fit a third time, where we restrict the fit to only the data in the range $-27\,000$ to -8000 km s^{-1} that completely avoids overlap with the C IV and Si IV BELs. In this case, the resulting slope is $-1.46 \pm 0.54 \times 10^{-5}$ fraction per km s^{-1}, which is non-zero at a 2.7σ significance. Therefore, this trend is evident even when we remove the data at the lowest and highest velocities, where additional uncertainty from the BELs can affect the results.

An important question is whether the trend seen in Fig. 3 is a correlation with velocity in an absolute sense or the cumulative result of differences between the red-side versus blue-side behaviours in individual absorption troughs. To address this question, we divided the velocity range of absorption for each quasar into a red and a blue half and plotted the incidence of variability separately for the red and blue portions. The result in both cases is consistent with the behaviour shown in Fig. 3. We do not see a higher incidence of variability in the blue portions of troughs versus the red portions. This indicates that the trend in Fig. 3 is a trend in the ensemble dependent on the absolute velocity rather than the relative velocity within a given trough. Consistent with this finding is the fact that none of the BALs varied at a velocity between -3500 km s^{-1} and 0 km s^{-1}, while both the two BALs in our sample at $< -33\,000$ km s^{-1} varied.

Another factor that might affect the results in Fig. 3 is that BALs at higher velocities tend to be weaker (Fig. 2). In Fig. 4, we examine C IV BAL variability as a function of absorption strength. Using the values of $\langle A \rangle$ calculated in Section 3, and a bin size of 0.05, we count how many quasars have absorption in each bin. We then count how many quasars have at least one occurrence of variability in each absorption strength bin. Each quasar is counted at most once in each

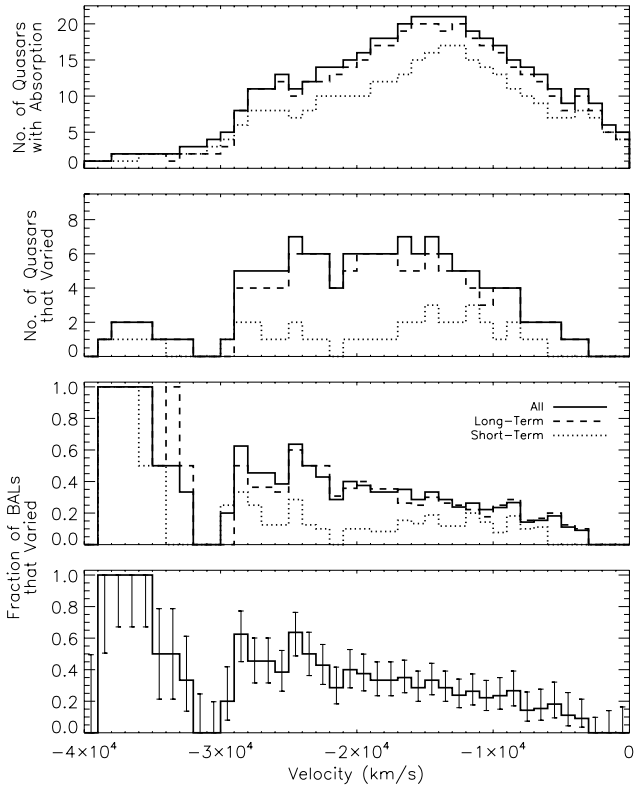

Figure 3. The top two panels show the number of quasars with C IV BAL absorption and the number with C IV BAL variability at each velocity. The third panel is the second panel divided by the top one, which gives the fraction of C IV BALs that varied at each velocity. The dashed, dotted and solid curves indicate results for the long-term, short-term and combined data set comparisons, respectively. The bottom panel displays the combined data set with 1σ error bars.

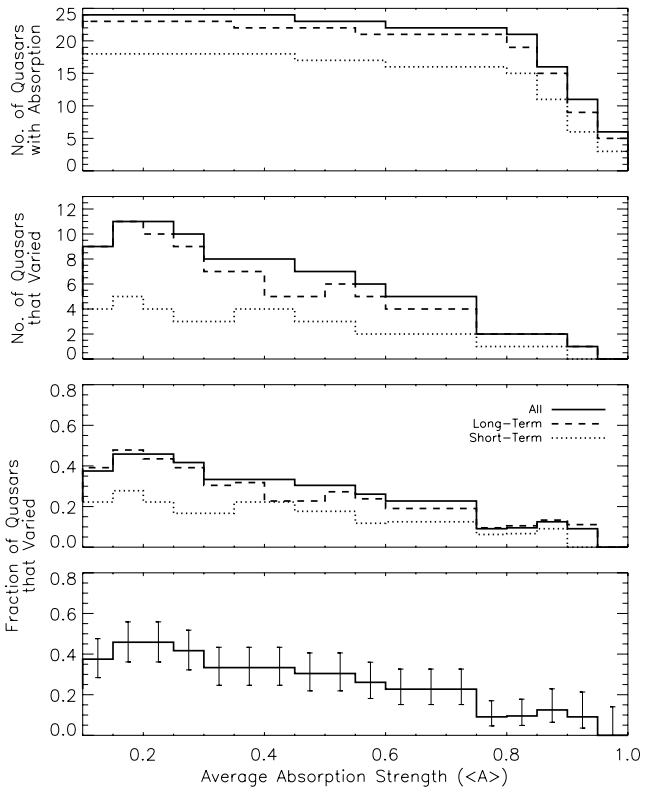

Figure 4. Same as Fig. 3, except the quantities are plotted as a function of the normalized absorption strength, averaged between the epochs being compared.

bin, even if it has the same absorption strength at more than one location in the spectrum. As in Fig. 3, the third panel is the second panel divided by the top one, in this case yielding the fraction of quasars with a BAL that varied in each absorption strength bin. Fig. 4 indicates that quasars are more likely to exhibit BAL variability at weaker absorption strengths. As in Fig. 3, we calculate errors for each absorption strength value. We again perform a least-squares fit, which gives a slope of -0.487 ± 0.095 fraction per unit absorption strength. The slope is non-zero at a 5σ significance. We repeat the least-squares fit with only the bins with the most data, as for Fig. 3; this restricts the fit to all of the bins except the one at $\langle A \rangle > 0.95$. The resulting slope is -0.476 ± 0.100 fraction per unit absorption strength, which is non-zero at a 4.8σ significance.

Fig. 4, however, does not account for multiple occurrences of the same absorption strength within an individual quasar. In Section 3.3, we define a method of dividing each BAL into $\sim$1200 km s^{-1} bins, and we now consider these bins as individual occurrences of absorption. In Fig. 5, we plot the number of these occurrences at each absorption strength value in the top panel and then the number of these occurrences that varied in the second panel. The third panel is the second panel divided by the top one, showing the fraction of occurrences at each absorption strength that varied. An individual BAL may be counted more than once at each absorption strength value because we consider portions of each BAL trough in this figure. The bottom panel is the same as the third panel, except it shows just the long-term data with error bars, calculated as in Figs 3 and 4. A least-squares fit for the long-term data in Fig. 5 gives a slope of -0.380 ± 0.052 fraction per unit absorption strength, which is non-zero at a 7σ significance. Fig. 5 confirms that weaker portions of BAL troughs are more likely to vary than stronger ones.

Figs 3–5 compare the *incidence* of variability to properties of the BALs. Next, we use the values of $|\Delta A|/\langle A \rangle$, calculated in Section 3, to compare the *amplitude* of variability to the same BAL properties.

In Fig. 6, we plot this fractional change in absorption strength as a function of the outflow velocity, using bin sizes of 1000 km s^{-1} width, as in Fig. 3. In each velocity interval, the individual points represent variability in a different quasar. The average values of $|\Delta A|/\langle A \rangle$ for just the variable (non-zero) points in each bin are shown by the open squares. The asterisks show the average if the non-varying absorption intervals are included. This plot does not indicate a statistically significant trend between fractional change in absorption strength and the outflow velocity.

In Fig. 7, we plot the fractional change as a function of average normalized absorption strength, similar to Fig. 6. In this plot, however, individual quasars will contribute multiple times to the measurements at a given absorption strength if the quasar has variability in both the red and blue sides of an absorption trough and/or in multiple troughs. The individual points represent variability at different velocities in each quasar. The average of all the variable (non-zero) points in each bin are shown by the open squares, while the asterisks show the average $|\Delta A|/\langle A \rangle$ in each bin if non-varying absorption regions are included. This plot indicates that the fractional change in strength is greater in weaker features. However, the errors in the values of $|\Delta A|/\langle A \rangle$ are correlated with the values of $\langle A \rangle$. At an $\langle A \rangle$ of 0.15, the typical error values range from $\sim$0.11 to 0.33,

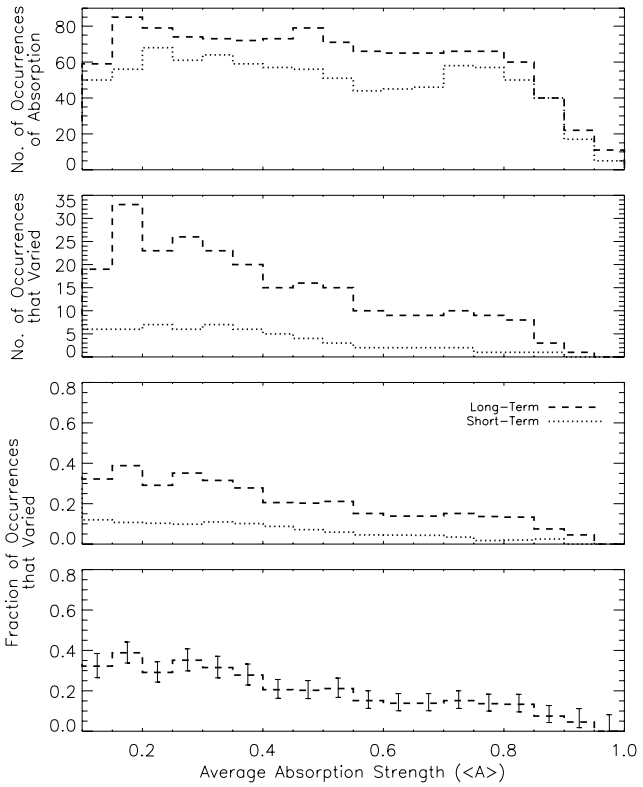

Figure 5. The top two panels show the total number of occurrences of absorption, and the number of those occurrences that varied, at each strength. The third panel is the second panel divided by the top one. The bottom panel displays the long-term data with 1σ error bars.

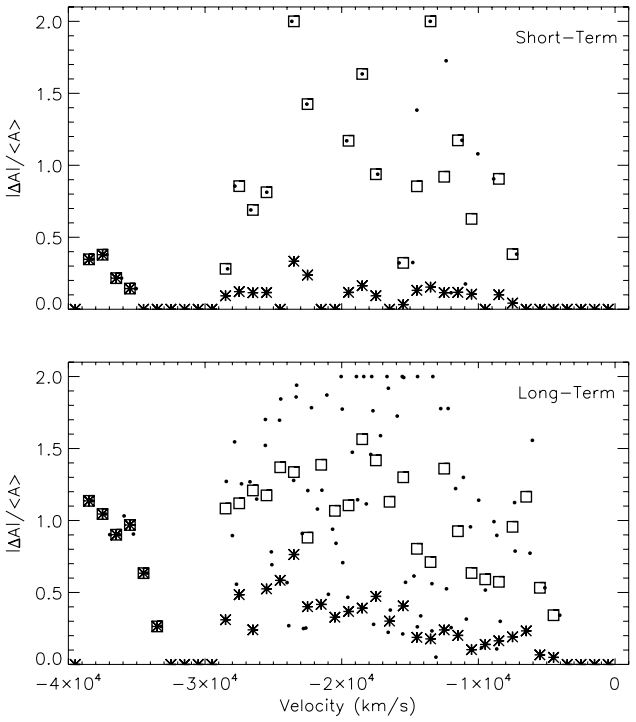

Figure 6. Fractional change in the depth of BAL absorption as a function of velocity. The symbols follow the same pattern as Fig. 2, with individual points representing variability in a single quasar. Here, the open squares indicate the average of these variable, non-zero points in each velocity bin. The asterisks show the average if the non-varying absorption intervals are included. The top panel shows the short-term results, while the bottom panel plots long-term data. We note that the maximum value of $|\Delta A|/\langle A \rangle$ is 2 (see Fig. 7), which indicates absorption appearing or disappearing completely.

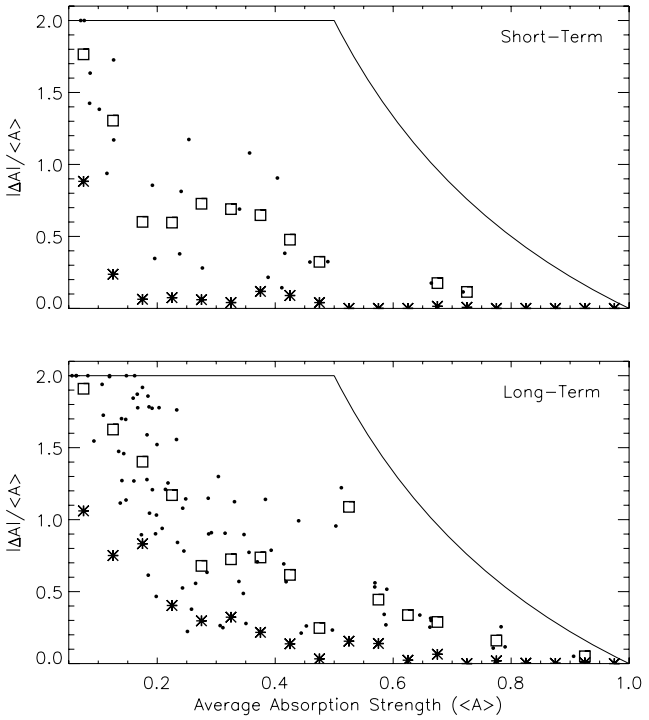

Figure 7. Same as Fig. 6, except the fractional change is now plotted as a function of average normalized absorption strength. In this plot, individual quasars can contribute multiple times to the measurements at a given absorption strength. The solid curve represents the maximum possible value of $|\Delta A|/\langle A\rangle$.

whereas at $\langle A\rangle$ of 0.60, the error values are ∼0.02–0.06. A larger error at smaller values of $\langle A\rangle$ should cause a larger dispersion in the points in that region of Fig. 7, but instead the values of $|\Delta A|/\langle A\rangle$ converge towards the maximum possible value of $|\Delta A|/\langle A\rangle$. The dispersion of points due to errors in $|\Delta A|/\langle A\rangle$ alone cannot explain the trend in this figure. Instead, this figure indicates that we see weaker absorbers, or weaker portions of BALs, appear or disappear completely, but strong features do not typically appear or disappear over the time-scales that our data cover.

Beyond looking at trends with velocity and absorption strength, it is instructive to examine the relationship between these two parameters. Fig. 2 displays $\langle A\rangle$ as a function of velocity, revealing that these quantities are correlated. The lack of a clear trend in Fig. 6 is surprising given that weaker systems are more variable (Fig. 7) and they tend to appear more often at higher velocities (Fig. 2). Evidently, the correlation of $|\Delta A|/\langle A\rangle$ with absorption strength is stronger than the correlation with velocity. We also investigate how $|\Delta A|$ varies with velocity and with $\langle A\rangle$. We do not include the plots here, but we find no trend between $|\Delta A|$ and velocity or absorption strength.

We do not find any significant differences in the trends described above between the short-term and long-term data. The main difference is in the incidence of variability, 39 per cent in the short-term data versus 65 per cent in the long-term data. The long-term data also show slightly larger changes in absorption strength, i.e. $|\Delta A|$, compared to the short-term data. The average value of $|\Delta A|$ is 0.16 ± 0.08 in the short term and 0.22 ± 0.10 in the long term.

We also note again that we include two quasars (0302+1705 and 0846+1540) from the Lick sample (Barlow 1993) that are not technically BALs. However, these two objects do not significantly affect the results. If we omitted them, then the fraction of quasars with variability would be 35 per cent (6/17) in the short term and 67 per cent (14/21) in the long term. In the case of 0302+1705, it does not qualify as a BALQSO because its broad absorption feature is at low velocities (centred at $\sim -2100\,\mathrm{km\,s^{-1}}$). It also has $\langle A\rangle$ reaching >0.90. It is a strong feature at low velocity that does not vary, fitting the trends discussed above. In 0846+1540, there is broad absorption at low velocity (centred at $\sim -2900\,\mathrm{km\,s^{-1}}$), with average $\langle A\rangle$ of ∼0.27, and at high velocity (centred at $\sim -26\,800\,\mathrm{km\,s^{-1}}$), with average $\langle A\rangle$ of ∼0.18. This also fits the overall trend for higher incidence of variability at higher velocities.

5 SUMMARY AND DISCUSSION

We have analysed short-term and long-term C IV λ1549 BAL variability in a sample of 24 quasars, and we looked for trends with the outflow velocity and absorption strength. We found that 39 per cent (7/18) of the quasars varied in the short term, intervals of 0.35–0.75 yr, whereas 65 per cent (15/23) varied in the long term, intervals of 3.8–7.7 yr. Overall, 67 per cent (16/24) of the quasars varied. We find a trend for variability to occur more often at higher velocities (Fig. 3) and in shallower absorption troughs (or shallower portions of absorption troughs; Figs 4 and 5). When looking at the fractional change in strength of the varying absorption features, there is no apparent significant correlation with velocity (Fig. 6), but there is a trend for a larger fractional change in absorption strength in shallower features (Fig. 7). We do include two objects with BI = 0, but the variability in the broad absorption in these two quasars is consistent with the trends described above.

Gibson et al. (2008) studied C IV BAL variability on time-scales of $\Delta t \sim 3$–6 yr in 13 quasars with two epochs of data and found that 92 per cent (12/13) varied. This is larger than our overall percentage of 67 per cent. This is surprising because the selection criteria adopted by Barlow (1993) for the sample used here might be biased towards more variable sources (Section 2). Evidently, this bias is small or non-existent. The difference between our result and Gibson et al. (2008) might be due to the small numbers of objects studied and/or the more conservative approach we took for identifying variable absorption.

Lundgren et al. (2007), which is a study of BAL variability on time-scales of <1 yr, find an inverse correlation of fractional change in EW with average EW. While EW is a different calculation than our measure of absorption strength, $\langle A\rangle$, encapsulating the entire BAL profile in one number instead of considering separately the different profile regions (Section 3.3), this result is consistent with our findings that fractional change in $\langle A\rangle$ correlates with $\langle A\rangle$. Lundgren et al. (2007) also find no overall trend between fractional change in EW and outflow velocity, which is again consistent with our results. While not plotted here, we do not find a significant correlation between $|\Delta A|$ and velocity or absorption strength, which is consistent with the analysis of Gibson et al. (2008). Gibson et al. (2008) also calculate the change in absorption strength, with values concentrated in the range 0.15–0.25. We find an average value of $|\Delta A|$ for the long-term data of 0.22 ± 0.10.

Both Gibson et al. (2008) and Lundgren et al. (2007) comment on the lack of evidence for acceleration in the BAL features they study. We also find no evidence for acceleration in our sample. The BAL variations only involve the absorption trough growing deeper or becoming shallower. We note, however, that limits on the acceleration are difficult to quantify for BALs because, unlike narrower absorption lines, they do not usually have sharp features

to provide an accurate velocity reference. BALs also exhibit profile variability, which can shift the line centroid without necessarily corresponding to a real shift in the velocity of material in the outflow.

In this work, we compare two different time intervals, and we do not find a significant difference between the short-term and long-term data in the trends described in Section 4. However, the incidence of variability and the typical change in strength is greater in the long term than in the short term. This indicates that BALs generally experience a gradual change in strength over multiyear time-scales, as opposed to many rapid changes on time-scales of less than a year. This will be investigated more in a later paper where we will include all the epochs from our data set.

Variability has been investigated in other types of absorbers that are potentially related to BALs. Narayanan et al. (2004) and Wise et al. (2004) looked for variability ($\Delta t \sim 0.3$–6 yr) in low-velocity narrow absorption lines (NALs) and found that 25 per cent (2/8) and 21 per cent (4/19), respectively, of the NALs they studied varied. Rodríguez Hidalgo et al. (in preparation) examined variability in mini-BALs, which are absorption lines with widths larger than those of NALs and smaller than those of BALs. They observed C IV mini-BALs in 26 quasars on time-scales of ∼1–3 yr and found variability in 57 per cent of the sources. This number is similar to our result for BALs; however this comparison is complicated by a differing number of epochs and different time baselines.

Rodríguez Hidalgo et al. (in preparation) found no correlation between incidence of mini-BAL variability and absorption strength or outflow velocity. However, this comparison might be skewed by the fact that mini-BALs tend to be weaker than BALs. For example, none of the mini-BALs studied by Rodríguez Hidalgo et al. (in preparation) has depths $A > 0.6$, while some of the BAL features in our sample have $A \sim 1$. There are also differences in the velocity distributions. The mini-BAL distribution in Rodríguez Hidalgo et al. (in preparation) peaks at $\sim -20\,000\,\mathrm{km\,s^{-1}}$, whereas the distribution of BAL absorption in our data peaks at $-15\,000$ to $-12\,000\,\mathrm{km\,s^{-1}}$ (Fig. 3). More work is needed, e.g. with larger samples, to control for these differences in the absorption characteristics and compare BAL and mini-BAL variabilities on equal footing. Comparisons like that could provide valuable constraints on the physical similarities and relationship between BAL and mini-BAL outflows.

Two possibilities for the cause of BAL variability are the movement of gas across our line of sight and changes in ionization. We found a trend for lines at higher velocity to vary more often, which suggests movements of clouds since faster moving gas might vary more. Moreover, this is a global trend, dependent on velocity in an absolute sense, rather than relative velocity within a given trough. However, it is possible that the root cause of the variability is associated with the strength of the lines, and weaker lines happen to appear at higher velocities (see Fig. 2 and Korista et al. 1993). In either case, faster moving material tends to have lower optical depths or cover less of the continuum source. Measured values of $\langle A \rangle$ thus provide either a direct measure of optical depth or covering fraction in the case of saturated absorption. With the current results, we cannot yet disentangle the trends in velocity and $\langle A \rangle$ with certainty.

Evidence from BAL variability studies none the less supports an interpretation of varying covering factor. In addition to greater variability at higher velocities, we found changes over small portions of the BAL troughs, rather than entire BALs varying, which can be understood in terms of movements of substructures in the flows. Changes in the ionizing flux should globally change the ionization in the flow, and we would expect these changes to be apparent over large portions of the BAL profiles and not in just some small velocity range. Hamann et al. (2008) looked at the variation in the C IV and Si IV BALs in one quasar and found that the BALs were locked at roughly a constant Si IV/C IV strength ratio. They attribute this result to the movements of clouds that are optically thick in both lines. If the level of ionization is constant between observations or if $\tau \gg 1$, then the changes in absorption strength in our sample are directly indicative of changes in the covering fraction. We will examine the Si IV/C IV line ratio in our BAL data in a subsequent paper.

On the other hand, studies of NALs support the possibility of changes in ionization causing the line variability. Misawa et al. (2007) and Hamann et al. (2011) observed quasars where multiple NALs varied in concert, which suggests global changes in the ionization of the outflowing gas. If a change in ionization is causing the variability in the BAL outflows, then the optical depth (τ) of the BALs is changing. Features with lower optical depth are much more sensitive to changes in ionization than those with higher optical depth. The outflowing gas is presumably photoionized by the flux from the continuum source, and changes in the continuum flux could cause a change in the ionization of the outflowing gas. However, studies to date have not found a strong correlation between continuum variability and BAL variability (Barlow et al. 1992; Barlow 1993; Lundgren et al. 2007; Gibson et al. 2008), casting doubt on ionization changes causing BAL variability.

Finally, we use the bolometric luminosities of the quasars in our sample to derive characteristic time-scales of the flows for comparison to the observed time-scales. The bolometric luminosities for the quasars in our sample range from $\sim 2 \times 10^{46}$ to $3 \times 10^{47}\,\mathrm{erg\,s^{-1}}$, and the average is $\sim 7 \times 10^{46}\,\mathrm{erg\,s^{-1}}$. These values are based on the observed flux at 1450 Å (rest frame) in absolute flux-calibrated spectra from Barlow (1993), a cosmology with $H_0 = 71\,\mathrm{km\,s^{-1}\,Mpc}$, $\Omega_\mathrm{M} = 0.3, \Omega_\Lambda = 0.7$ and a standard bolometric correction factor $L \approx 4.4\lambda\ L_\lambda(1450\,\text{Å})$. Based on the average value of $L \sim 7 \times 10^{46}\,\mathrm{erg\,s^{-1}}$, a characteristic diameter for the continuum region at 1550 Å is $D_{1550} \sim 0.006$ pc and for the C IV BEL region is $D_\mathrm{C\,IV} \sim 0.3$ pc, assuming $L = 1/3 L_\mathrm{edd}$ and $M_\mathrm{BH} = 1.4 \times 10^9\,\mathrm{M_\odot}$ (Peterson et al. 2004; Bentz et al. 2007; Gaskell 2008; Hamann & Simon, in preparation). If the outflowing gas is located just beyond the C IV BEL region and it has a transverse speed equal to the Keplerian disc rotation speed, then the gas cloud would cross the entire continuum source in ∼1 yr. The typical time-scale in our short-term data is ∼0.5 yr, and the typical change in absorption strength is at least 10 per cent, which nominally requires the moving clouds to cross at least 10 per cent of the continuum source. This implies transverse speeds $>1000\,\mathrm{km\,s^{-1}}$, and thus radial distances that are conservatively <6 pc if the transverse speeds do not exceed the Keplerian speed. A typical time-scale in the long-term data is ∼6 yr, which is enough time to cross the continuum source approximately seven times (if the gas is located just beyond the C IV BEL region). This suggests a fairly homogeneous flow for at least the cases where there is no long-term variability.

To place better constraints on the outflow properties and understand the underlying cause(s) of the line variabilities, our following papers will make more complete use of our entire data sample. We will examine the ratio of Si IV to C IV absorption to gain better insight into the cause(s) of the variability, and we will utilize more complete time sampling instead of just looking at two specific ranges of time intervals. We have also obtained more data on BAL variability at the shortest time-scales, $\Delta t \sim 1$ week to 1 month, in order to determine whether there is a minimum time-scale over

which variability occurs. This will provide a better constraint on the location of the outflowing gas.

ACKNOWLEDGMENTS

We thank an anonymous referee for helpful comments on the manuscript. Funding for the SDSS and SDSS-II has been provided by the Alfred P. Sloan Foundation, the Participating Institutions, the National Science Foundation, the US Department of Energy, the National Aeronautics and Space Administration, the Japanese Monbukagakusho, the Max Planck Society and the Higher Education Funding Council for England. The SDSS website is http://www.sdss.org/.

REFERENCES

Adelman-McCarthy J. K. et al., 2008, ApJS, 175, 297
Agresti A., Coull B. A., 1998, American Statistician, 52, 119
Barlow T. A., 1993, PhD thesis, Univ. California, San Diego
Barlow T. A., Junkkarinen V. T., Burbidge E. M., Weymann R. J., Morris S. L., Korista K. T., 1992, ApJ, 397, 81
Bentz M. C., Denney K. D., Peterson B. M., Pogge R. W., 2007, in Ho L. C., Wang J.-M., eds, ASP Conf. Ser. Vol. 373. The Central Engine of Active Galactic Nuclei. Astron. Soc. Pac., San Francisco, p. 380
Di Matteo T., Springel V., Hernquist L., 2005, Nat, 433, 604
Everett J. E., 2005, ApJ, 631, 689
Gaskell C. M., 2008, Rev. Mex. Astron. Astrofis., 32, 1
Gibson R. R., Brandt W. N., Schneider D. P., Gallagher S. C., 2008, ApJ, 675, 985
Gibson R. R., Brandt W. N., Gallagher S. C., Hewett P. C., Schneider D. P., 2010, ApJ, 713, 220
Hamann F., Barlow T. A., Junkkarinen V., Burbidge E. M., 1997, ApJ, 478, 80
Hamann F., Kanekar N., Prochaska J.-X., Murphy M.-T., Ellison S., Malec A.-L., Milutinovic N., Ubachs W., 2011, MNRAS, 410, 1957
Hamann F., Kaplan K. F., Hidalgo P. R., Prochaska J. X., Herbert-Fort S., 2008, MNRAS, 391, L39
Korista K. T., Voit G. M., Morris S. L., Weymann R. J., 1993, ApJS, 88, 357
Lundgren B. F., Wilhite B. C., Brunner R. J., Hall P. B., Schneider D. P., York D. G., Vanden Berk D. E., Brinkmann J., 2007, ApJ, 656, 73
Misawa T., Eracleous M., Charlton J. C., Kashikawa N., 2007, ApJ, 660, 152
Moll R. et al., 2007, A&A, 463, 513
Murray N., Chiang J., Grossman S. A., Voit G. M., 1995, ApJ, 451, 498
Narayanan D., Hamann F., Barlow T., Burbidge E. M., Cohen R. D., Junkkarinen V., Lyons R., 2004, ApJ, 601, 715
Peterson B. M. et al., 2004, ApJ, 613, 682
Proga D., 2007, ApJ, 661, 693
Proga D., Kallman T. R., 2004, ApJ, 616, 688
Reichard T. A. et al., 2003a, AJ, 125, 1711
Reichard T. A. et al., 2003b, AJ, 126, 2594
Shen Y., Strauss M. A., Hall P. B., Schneider D. P., York D. G., Bahcall N. A., 2008, ApJ, 677, 858
Trump J. R. et al., 2006, ApJS, 165, 1
Vanden Berk D. E. et al., 2001, AJ, 122, 549
Weymann R. J., Morris S. L., Foltz C. B., Hewett P. C., 1991, ApJ, 373, 23
Wilhite B. C., Vanden Berk D. E., Kron R. G., Schneider D. P., Pereyra N., Brunner R. J., Richards G. T., Brinkmann J. V., 2005, ApJ, 633, 638
Wilson E. B., 1927, J. American Statistical Association, 22, 209
Wise J. H., Eracleous M., Charlton J. C., Ganguly R., 2004, ApJ, 613, 129

This paper has been typeset from a TEX/LATEX file prepared by the author.